Supplementary file for

Seismic Moment Efficiency Reveals the Potential for Larger Earthquakes After M6-Class Events

Satoshi Matsumoto[1]*, Koki Aizawa[1], Takeshi Matsushima

Corresponding author: matumoto@sevo.kyushu-u.ac.jp

The PDF file includes:

Extended Data Figs. 1 to 6 and Tables 1 to 2

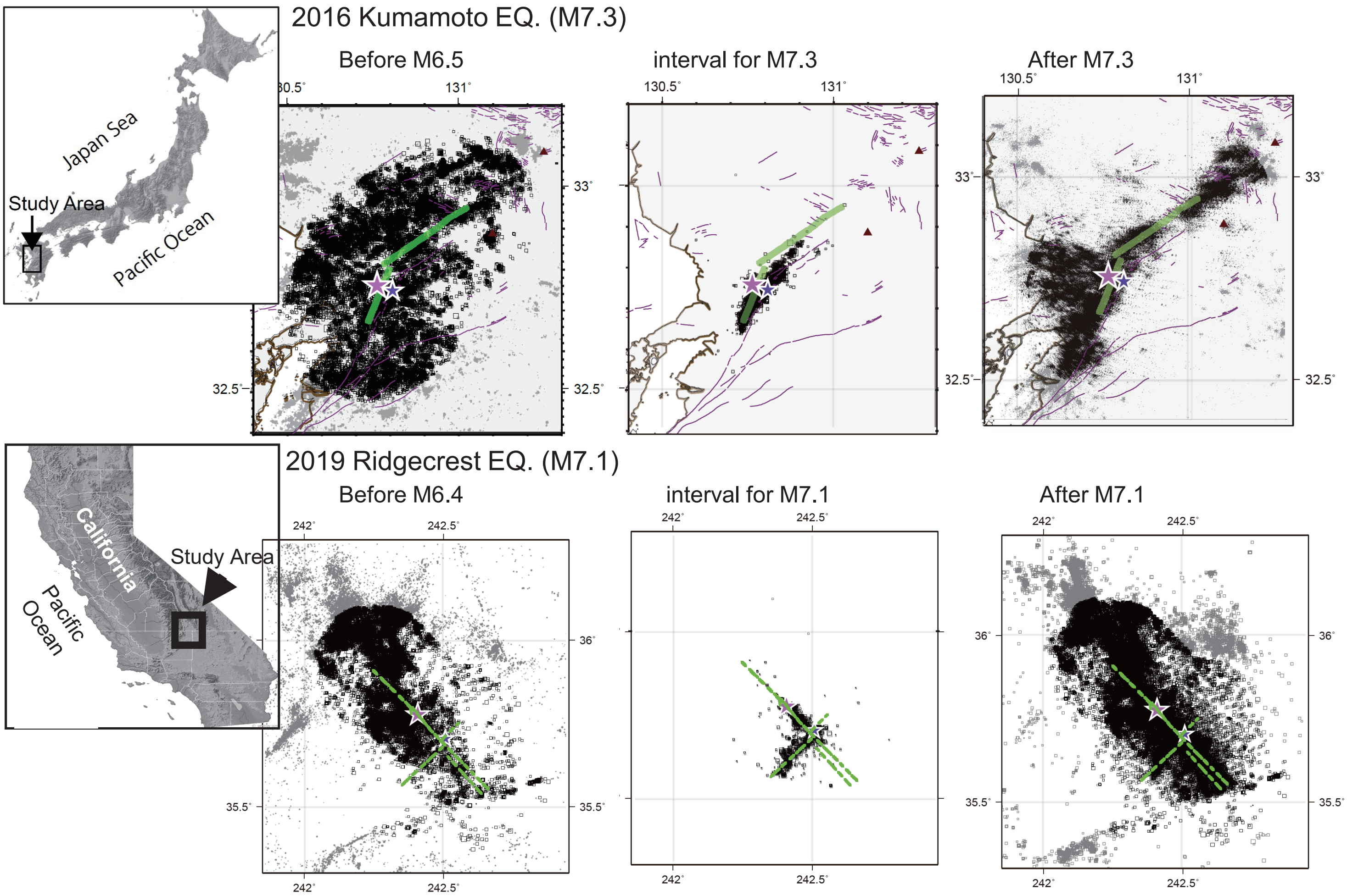

Extended data Fig. 1 Epicenter distributions around the 2016 Kumamoto and 2019 Ridgecrest earthquake faults. Circles in black and gray indicate hypocenters located within 20 km of the earthquake faults (shown as green segments) and those located furth away, respectively. Large and small stars represent the mainshock and the largest foreshock. The distributions correspond to the periods before the largest foreshock (Bef.), during the interval period leading up to the mainshock (Int.), and after the mainsho ck (Aft.), respectively. Green segments indicate coseismic fault trace at depth range of 10 – 11 km modeled by the previous studies[21,22].

Extended data Table 1. Numbers of events and focal mechanisms.

	before		interval		after	
	Hypocenter	Mechanism	Hypocenter	Mechanism	Hypocenter	Mechanism
2016 Kumamoto	33550	2742	2129	881	129389	6578
2019 Ridgecrest	78774	13736	1813	1193	52150	29734

The hypocenters located within 20 km of the earthquake faults and in the depth range of 0 – 20 km. The values are before the largest foreshock (Bef.), during the interval period leading up to the mainshock (Int.), and after the mainshock (Aft.)

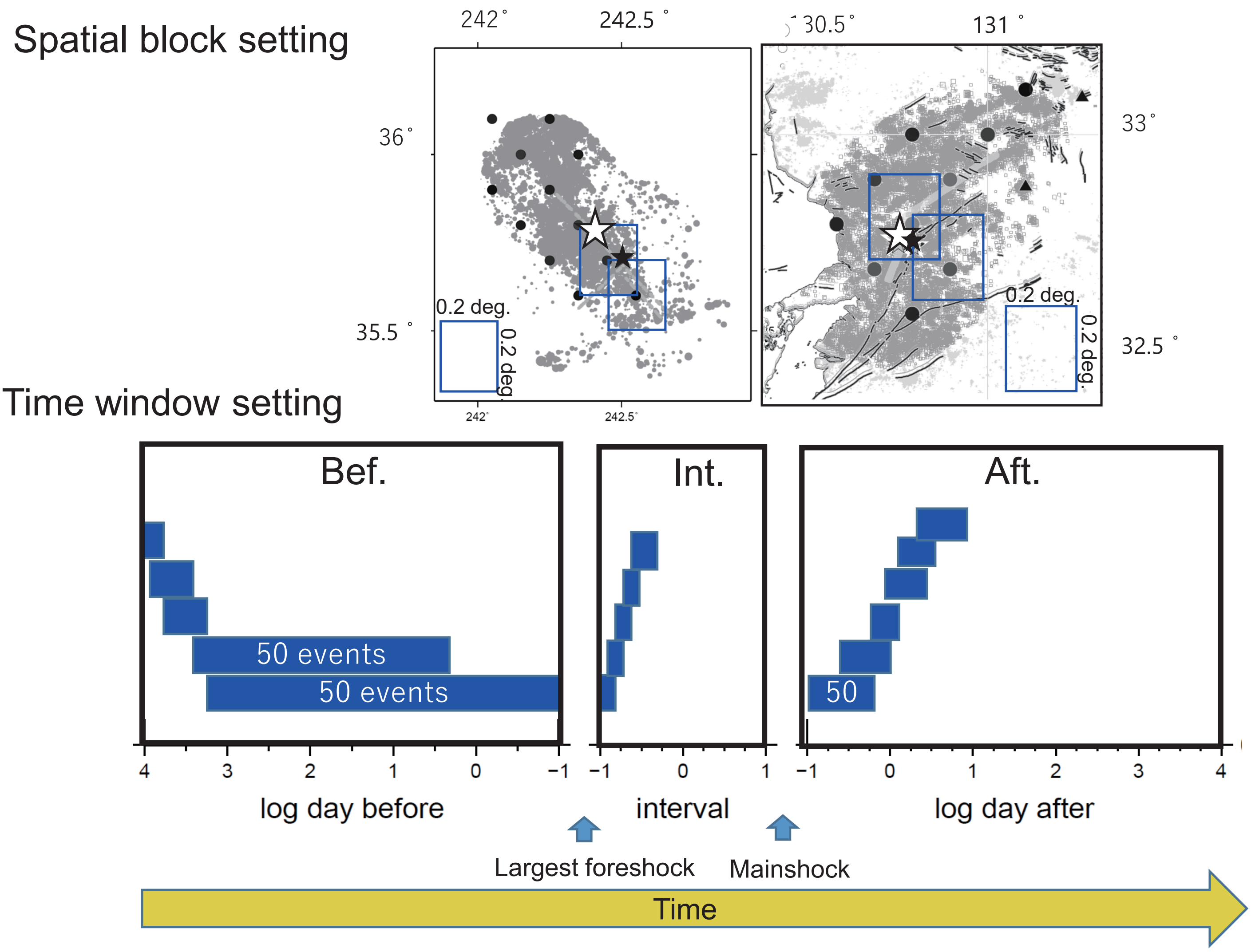

Extended Data Fig. 2 Schematic illustrations of spatial binning and time window settings.

Top: Spatial bins are defined across the target sequence area, each covering 0.2° in horizontal extent and depths from 0 to 20 km. An additional secondary grid, offset by 0.1 horizontally, is also used. Solid circles indicate the center of each spatial bin, and the blu rectangle shows an example of a bin area.

Bottom: Time windows are constructed using 50 sequential events within each spatial bin, with a 25-event overlap between consecutive windows. For the Bef. period, events are counted in reverse chronological order from the largest foreshock. Each **M_{stk}/M_0** value is plotted at the temporal midpoint of its corresponding 50-event window, as shown in Fig. 1 and Extended Data Fig.6. the midpoint time of each event group. The horizontal axis represents time in logarithmic scale. For the Bef. period, time is measured backwar from the largest foreshock; for the Int. period, it is measured forward from the same foreshock. For the Aft. period, time is measured forward from the mainshock. The zero point on the axis corresponds to one day after each respective reference event (i.e., the largest foreshock or the mainshock).

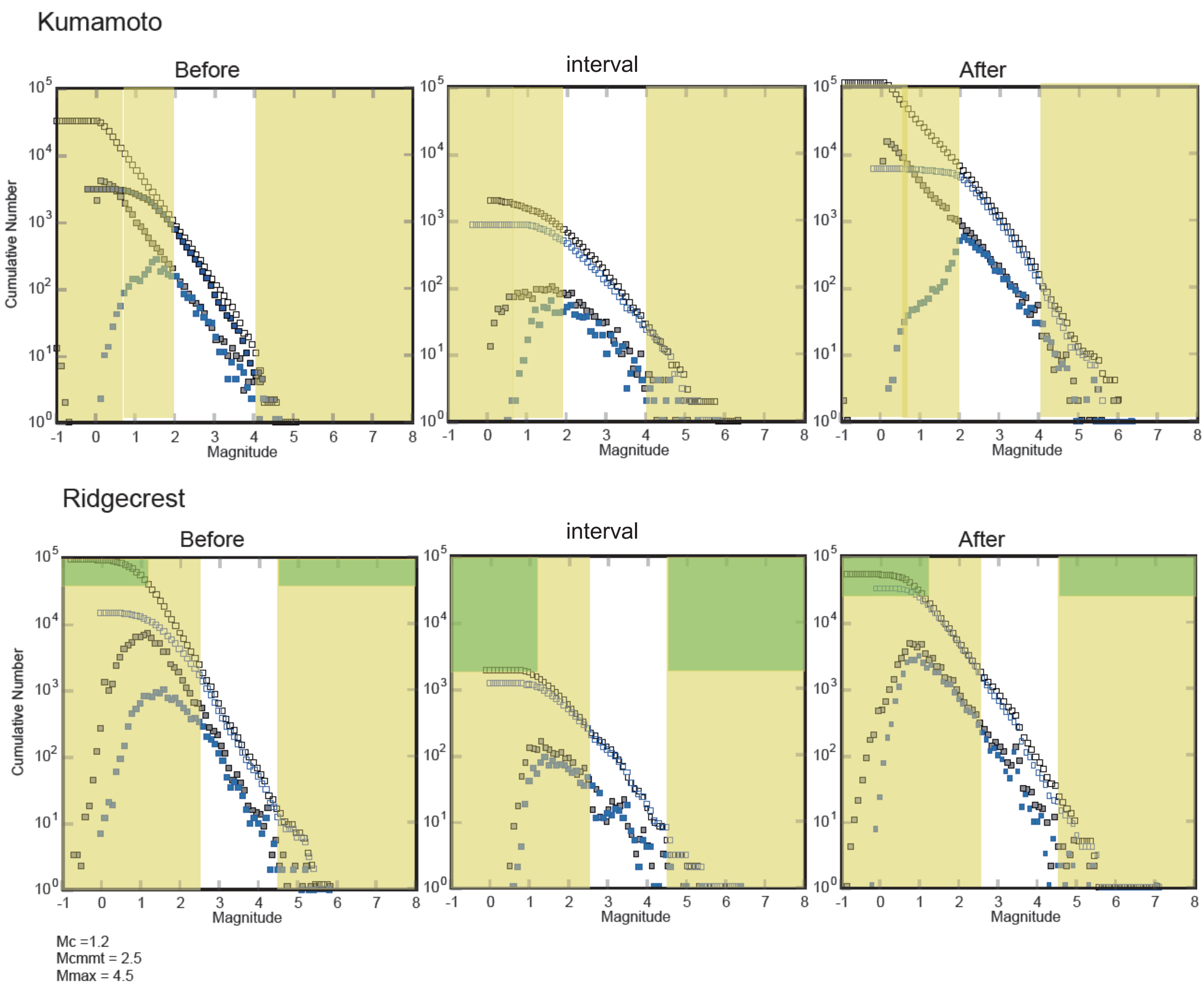

Extended Data Fig.3 Frequency-Magnitude distribution The upper and lower panels show results for the 2016 Kumamoto and 2019 Ridgecrest sequences, respectively. Cumulative and individual event counts within each magnitude bin are shown using open and solid symbols, respectively.

Blue symbols indicate events with available focal mechanism solutions. The unshaded area represents the magnitude range used for **M**stk/**M**$_0$ estimation. The green-hatched area indicates the excluded range for b-value estimation in the Ridgecrest data

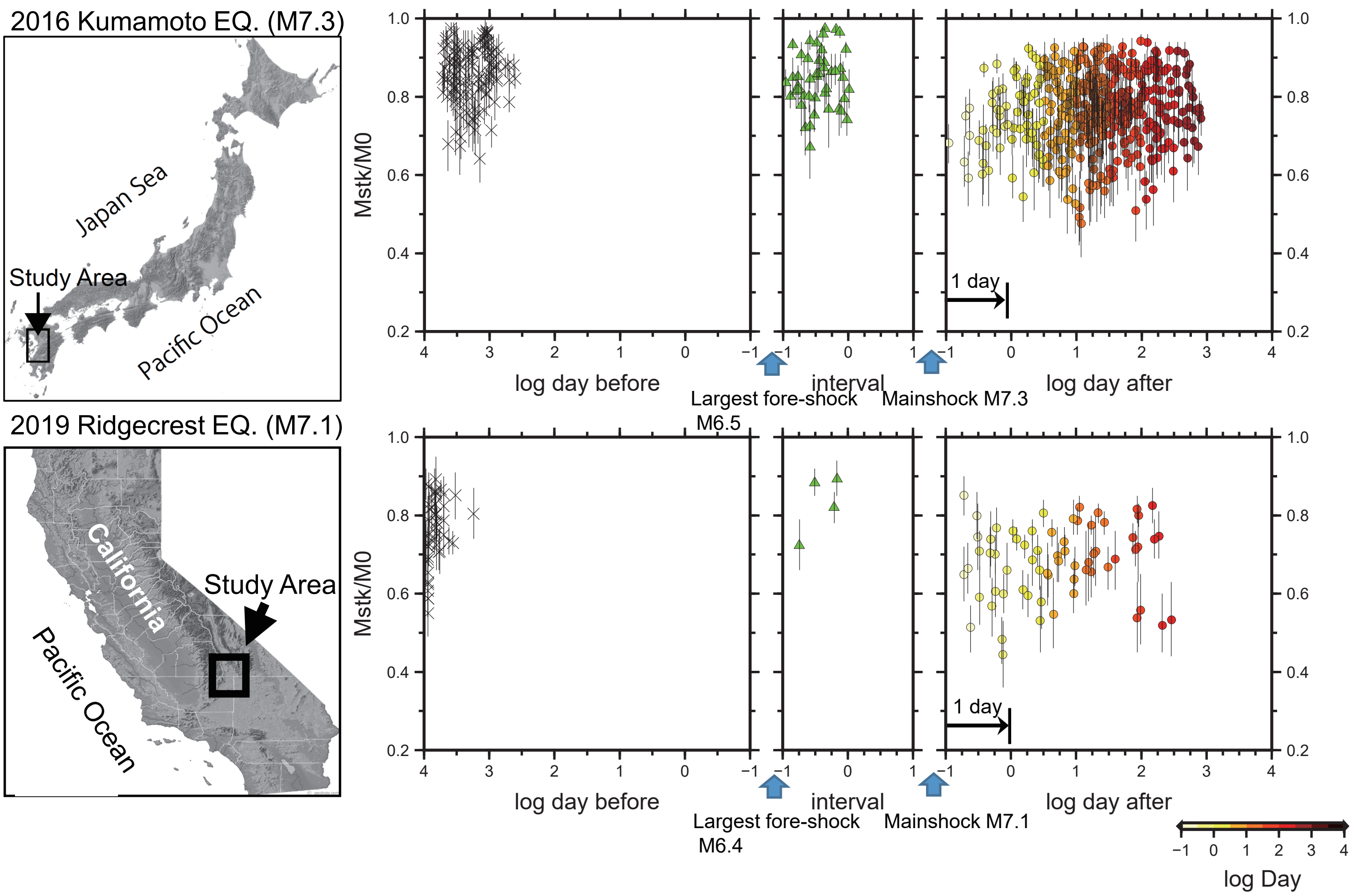

Extended Data Figure 4. Temporal variations of Mstk/M$_0$ before (Bef.), during (Int.) and after (Aft.) the mainshock for 0.1 x 20km spatial bin

Same Figure as Figure 1 except spatial bin size of 0.1° × 20 km. Upper and lower panels show the 2016 Kumamoto and 2019 Ridgecrest sequences, respectively (locations in ins maps). Crosses, triangles, and circles indicate **Mstk/M$_0$** values for Bef., Int., an d Aft. periods, based on 50 sequential events within a spatial bin. For Bef., events are counted backward from the largest foreshock ; for the Int. period, forward from the same event; and for the Aft. period, forward from the mainshock Each value is plotted at the temporal midpoint of its corresponding event group. The magnitude range is 2 – 4 for Kumamoto and 2.5 – 4.5 for Ridgecrest areas. Time is shown on a logarithmic scale, where zero corresponds to one day after each respective reference event. Vertical bars indicate bootstrap-estimated standard errors. In Aft., symbol color shows days since the mainshock (log scale).

Extended Data Table 2. Changes in Mstk/M_0 across different periods.

Earthquake	Before			After (1 day)			Note
	Mstk/ M0	err	Ntw	Mstk/ M0	err	Ntw	
2018 N. Osaka M6.1	0.755	0.013	48	0.778	0.042	7	
2018 W. Shimane M6.1	0.827	0.015	38	0.812	0.027	13	
2016 E. Tottori M6.6	0.858	0.012	41	0.729	0.020	21	
2014 N. Nagano M6.7	0.813	0.033	15	0.647	0.053	5	
2013 N. Tochigi M6.3	0.762	0.020	24	0.677	0.040	8	
2011 Fukushima-Ibaraki M6.1	0.741	0.040	2	0.728	0.050	10	M7.0 (22 days after)
2011 Mt. Fuji M6.4	0.800	0.079	3	0.579	0.089	1	
2008 Iwate-Miyagi M7.2	0.748	0.069	3	0.604	0.048	9	
2004 Mid Niigata M6.8	0.501	0.143	1	0.695	0.039	8	
2019 Ridgecrest M6.1	0.785	0.008	87	0.802	0.032	9	M7.1 (34 hrs. after)
2016 Kumamoto M6.5	0.813	0.017	16	0.851	0.012	35	M7.3 (27 hrs. after)

This table lists values for Kumamoto and Ridgecrest sequences and all large inland earthquakes (M > 6) in Japan from 2002 to 2020 that were preceded by seismic activity. For each event, **Mstk/M_0** was calculated using earthquakes within 20 km of the hypocenter, using time windows defined in the same way as for the Kumamoto and Ridgecrest sequences. A weighted average of **Mstk/M_0** was computed across the time windows using inverse-variance weighting, with weights set to the reciprocal of the estimated variance for each window. The "err" column indicates the propagated uncertainty derived from the variances of **Mstk/M_0** across the windows. "Ntw" refers to the number of time windows used in the weighted average. "1 day" represent the respective durations over which the averaging was performed. For events that were followed by an even larger earthquake, the magnitude and time elapsed until that subsequent event are noted in the "Note" column.

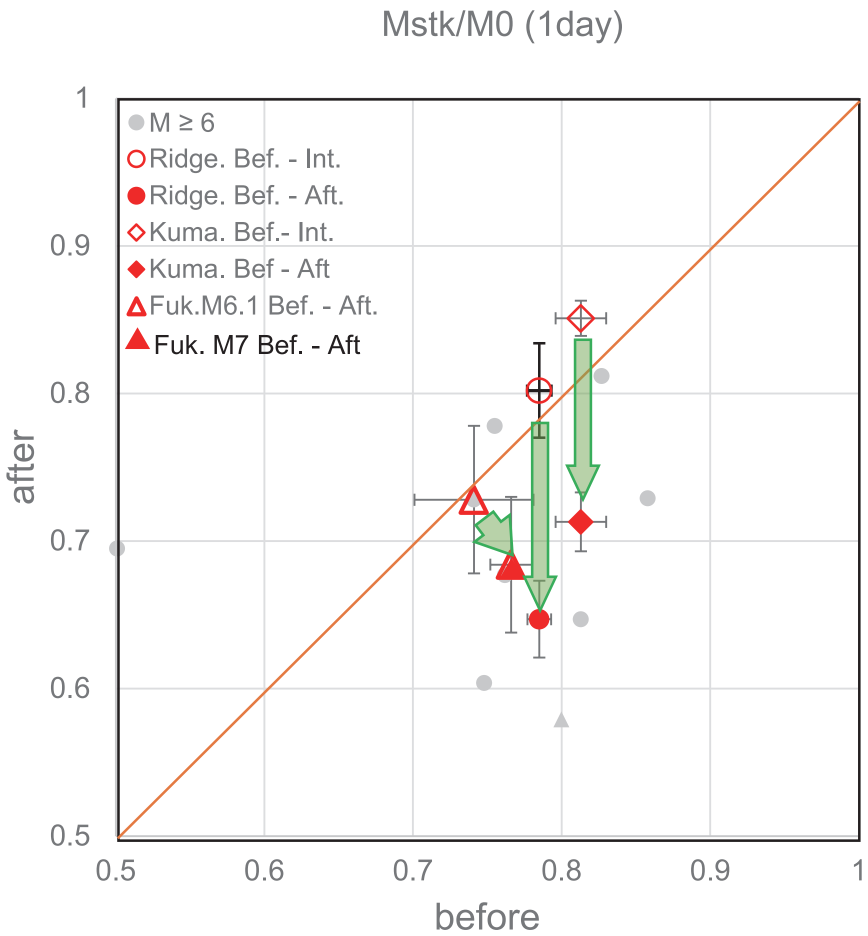

Extended Data Figure 5. Mstk/M₀ before and after large earthquakes (M ≥ 6).
Same as Figure 2, but includes additional data for the Bef.–Aft. period for events followed by an even larger earthquake. Open symbols represent **Mstk/M₀** values within 1 day after versus before each M ≥ 6 earthquake. Solid symbols highlight cases that were followed by an even larger event.
For the Fukushima–Ibaraki M6.1–M7 sequence (Fuk.), the Bef.–Aft. **Mstk/M₀** value (solid triangle) was computed from the data within 1 day before and after the M7 mainshock. Gray circles indicate events already plotted in Figure 2. Green arrows show changes in **Mstk/M₀** between the two periods for the Kumamoto (Kuma.), Ridgecrest (Ridge.), and Fukushima–Ibaraki (Fuk.) sequences.

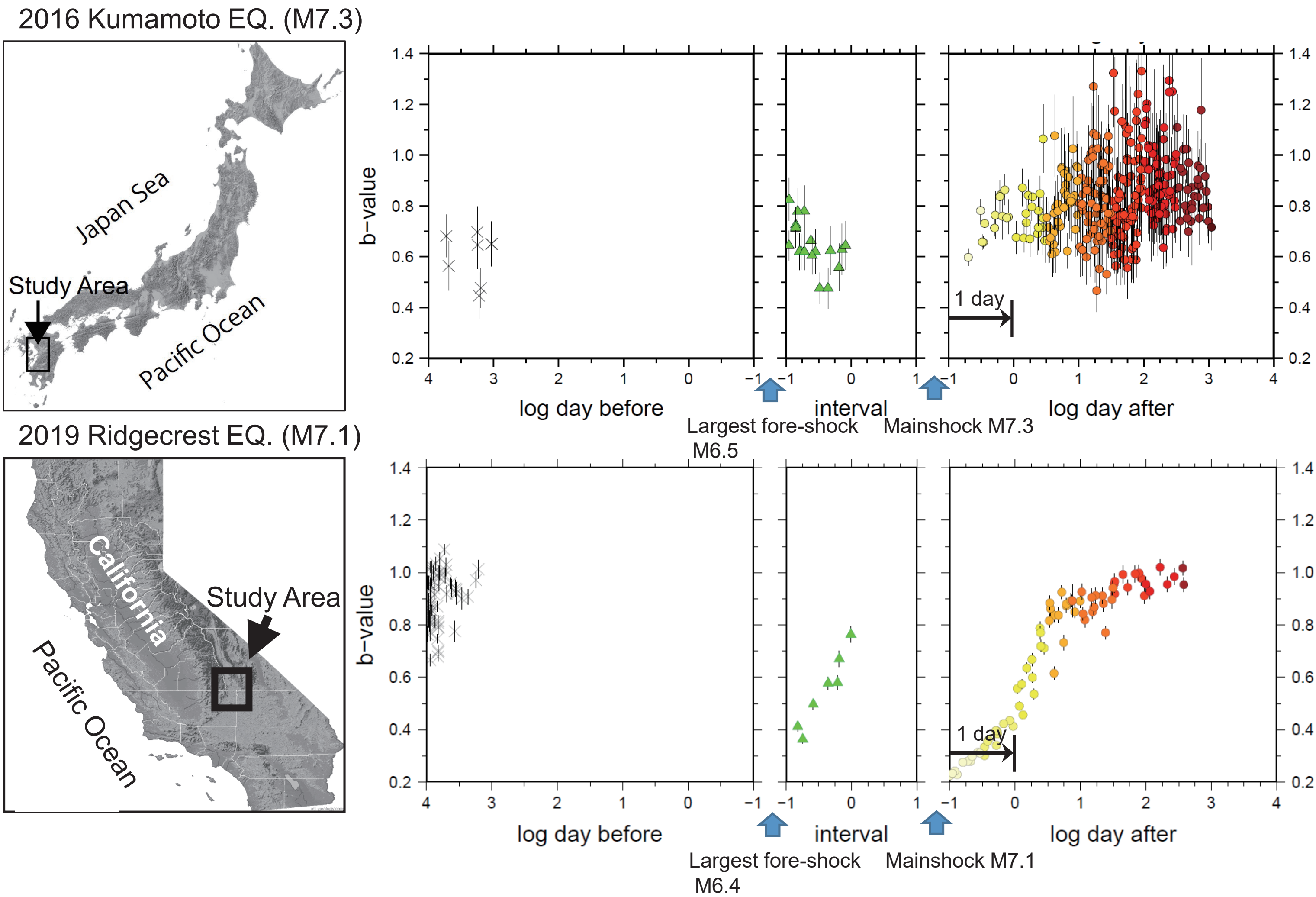

Extended Data Fig. 6. Temporal variations in b-values before, during, and after major earthquakes.

Panels show b-values before the largest foreshock (Bef.), during the interval leading to the mainshock (Int.), and after the mainshock (Aft.). The upper and lower panels correspond to the 2016 Kumamoto and 2019 Ridgecrest sequences, respectively; their locations are shown in the inset maps.

Crosses, triangles, and circles represent b-values for the Bef., Int., and Aft. periods. Each value is calculated using the same time windows as those used for **M**stk/**M**₀ in Fig. 1. The magnitude ranges are 2–4 for Kumamoto and 1.2–4.5 for Ridgecrest.

The horizontal axis indicates the midpoint of each time window. Vertical bars show standard error ranges estimated using the maximum likelihood method. In the Aft. panel, symbol color corresponds to the logarithmic time since the mainshock, as indicated by the color scale.